MAUSAM, **71**, 3 (July 2020), 405-422

551.577 : 551.509.3 (548.7)

Impacts of the Madden-Julian Oscillation (MJO) on rainfall in Sri Lanka

I. M. SHIROMANI PRIYANTHIKA JAYAWARDENA, MATTHEW C. WHEELER*,
W. L. SUMATHIPALA** and B. R. S. B. BASNAYAKE***
Department of Meteorology, Sri Lanka
**Bureau of Meteorology, Melbourne, Victoria, Australia*
***Ministry of Environment / The Open University of Sri Lanka*
****Asia Disaster Preparedness Center, Bangkok, Thailand*
(*Received 4 September 2019, Accepted 3 March 2020*)
e mail : shirojaya2000@yahoo.com

सार – श्रीलंका में वर्षा पर मैडेन जूलियन ऑसिलेशन (एम.जे.ओ.) के प्रभाव की जांच 1981-2010 तक के 30 वर्षों के दैनिक स्टेशन के आँकड़ों के आधार पर की गई है। एम.जे.ओ. के आठ चरणों में से प्रत्येक के लिए वास्तविक समय बहु परिवर्तनशील एम.जे.ओ. (आर.एम.एम.) सूचकांक के साथ परिभाषित करके कंपोजिट्स तैयार किए गए हैं, जिसके लिए चार जलवायविक ऋतुओं में श्रीलंका के 44 स्टेशनों से दैनिक वर्षा के आँकड़ों का उपयोग किया गया है और उपग्रह पर आधारित वर्षा के समान परिणामों की तुलना की गई है। स्थानीय वर्षा विसंगतियाँ बड़े पैमाने पर परिसंचरण के साथ कैसे संबद्ध होती हैं, इसका पता लगाने के लिए निम्न क्षोभमंडलीय पवन और संवहन विसंगति के कंपोजिट की भी जांच की गई है। श्रीलंका में वर्षा पर एम.जे.ओ. का सबसे अधिक प्रभाव द्वितीय अंतर-मॉनसून (एस.आई.एम.) और दक्षिण-पश्चिमी मॉनसून (एस.डब्ल्यू.एम.) ऋतुओं में होता है। श्रीलंका में आर.एम.एम. के दूसरे और तीसरे चरणों के दौरान, जब एम.जे.ओ. संवहन आवरण हिंद महासागर में स्थित होता है, तब आमतौर पर अधिक वर्षा होती है, और इसके विपरीत छठवें और सातवें चरण में वर्षा में कमी होती है। वर्षा का उक्त प्रभाव श्रीलंका के आस-पास एम.जे.ओ. की उष्णकटिबंधीय संवहन विसंगतियों और संबद्ध निचले स्तर के परिसंचरण के प्रत्यक्ष प्रभाव के कारण होता है। इसके विपरीत, उत्तरी शीतकाल के दौरान एम.जे.ओ. संवहनी आवरण के दक्षिणवर्ती विस्थापन के परिणामस्वरूप पूर्वोत्तर मॉनसून (एन.ई.एम.) ऋतु के दौरान एम.जे.ओ. का प्रभाव दक्षिण-पश्चिमी मॉनसून और द्वितीय अंतर-मॉनसून (एस.आई.एम.) ऋतु की तुलना में कुछ कम होता है। चरम वर्षा की घटनाएं प्रथम अंतर-मॉनसून (एफ.आई.एम.) के दूसरे चरण में और दक्षिण-पश्चिमी मॉनसून के दूसरे और तीसरे चरणों, द्वितीय अंतर-मॉनसून (एस.आई.एम.) के पहले, दूसरे और तीसरे चरणों और उत्तर-पूर्वी मॉनसून ऋतु के दूसरे और तीसरे चरणों के दौरान सबसे अधिक होती हैं। इस अध्ययन के विश्लेषण से एक उपयोगी संदर्भ मिलता है कि श्रीलंका में चार जलवायविक ऋतुओं के दौरान वर्षा के साथ-साथ चरम वर्षा की घटनाओं पर एम.जे.ओ. का कब और कहाँ महत्वपूर्ण प्रभाव पड़ा है। श्रीलंका में विस्तारित अवधि पूर्वानुमान को और बेहतर बनाने के लिए, गतिकीय या सांख्यिकीय मॉडलों द्वारा सटीक रूप से अनुमानित एम.जे.ओ. चरण के साथ इस जानकारी का उपयोग किया जा सकता है।

ABSTRACT. The influence of the Madden Julian Oscillation (MJO) on rainfall in Sri Lanka (SL) is examined based on 30 years of daily station data from 1981-2010. Composites are constructed for each of the eight phases of the MJO defined with the Real-time Multivariate MJO (RMM) index, using daily rainfall data from 44 stations over SL for four climatic seasons and comparing to similar results from a satellite-based rainfall product. Composites of lower tropospheric wind and convective anomaly are also investigated in order to examine how the local rainfall anomalies are associated with large-scale circulations. The greatest impact of the MJO on rainfall over SL occurs in the Second Inter-Monsoon (SIM) and Southwest Monsoon (SWM) seasons. Enhanced rainfall generally occurs over SL during RMM phases 2 and 3 when the MJO convective envelop is located in the Indian Ocean and conversely suppressed rainfall in phases 6 and 7. This rainfall impact is due to the direct influence of the MJO's tropical convective anomalies and associated low-level circulations in the vicinity of SL. In contrast, the MJO influence during the Northeast Monsoon (NEM) season is slightly less than during the SWM and SIM seasons as a result of the southward shift of the MJO convective envelop during boreal winter. Occurrence of extreme rainfall events is most frequent during phase 2 in First Inter-Monsoon (FIM) phases 2 and 3 in SWM, phases 1, 2 and 3 in SIM and phases 2 and 3 in NEM seasons. The analysis of this study provides a useful reference of when and where the MJO has significant impacts on rainfall as well as extreme rainfall events during four climatic seasons in SL. This information can be used along with accurately predicted MJO phase by dynamical or statistical models, to improve extended range forecasting in SL.

Key words – Madden Julian Oscillation, Monsoon, Inter-monsoon, Rainfall variability.

1. Introduction

Sri Lanka (SL) is an island located in the tropics between 5° 55' to 9° 51' North latitude and between 79° 42' to 81° 53' East longitude. The country exhibits typical characteristics of tropical weather owing to its latitudinal position; on the other hand it is also a part of the South Asian monsoon climate region affected by both Southwest Monsoon (SWM) and Northeast Monsoon (NEM) seasons (Chandrapala, 1996). The two monsoons essentially determine the seasonality of SL since the temperature shows hardly any significant variation throughout the year. The seasons are distinguished only by means of the timing of the two monsoons and the transitional periods separating them, called inter-monsoon seasons (Chandrapala, 1996). Due to the near-equatorial location of SL, the Inter Tropical Convergence Zone (ITCZ) crosses twice a year during its migration, playing an important role in SL's rainfall distribution (Suppiah, 1996; Ding and Sikka, 2006). Consequently, SL's rainfall exhibits a marked seasonality in its spatial and temporal aspects (Suppiah, 1989). The annual rainfall shows [Fig. 3(e)] remarkable spatial variation, ranging from less than 1000 mm in the driest parts to more than 5000 mm in the wettest parts. The SWM contributed 30% of annual average rainfall ranging from 10-20% in dry zone to more than 50-65% over western slopes of the central hills [Fig. 3(a)] and the NEM contributed 26% ranging from 30-50% in north-eastern parts dry zone and 7.5-15% in wet zone to the annual average rainfall [Fig. 3(a)]. The inter-monsoon periods, namely First inter-monsoon (FIM) and Second Inter-monsoon (SIM) contributed 14% and 30% to annual average rainfall respectively [Fig. 3(a)].

The spatial patterns of the rainfall in different seasons indicate that the southwestern sector of the island receives the highest rainfall in all the seasons except in the NEM season, which makes it the zone of maximum rainfall in the annual rainfall pattern [Figs. 3(b&c)]. Thus, SL has been categorized in to three spatial climatic zones: the Wet Zone in the southwestern region including the western and southern slopes of the central hills; the Dry Zone covering predominantly the northern and eastern part of the country: and the Intermediate Zone, skirting the central hills except in the south and the west (Thambyahpillay, 1954). Three climatic zones are demarcated based on rainfall, soils and vegetation (Somasekeram *et al.*, 1988). The wet zone receives an annual rainfall of more than 2500 mm; the intermediate zone receives between 1750 and 2500 mm and the dry zone receives less than 1750 mm a year.

The agricultural activities, water resources management, hydropower generation and reservoir management in the country are highly susceptible to rainfall variability on the intra-seasonal timescale. Disease outbreaks such as Dengue, the most common vector borne disease in SL, are also sensitive to rainfall variability on the intra-seasonal timescale. Therefore, the understanding of intra-seasonal rainfall variability and its prediction are essential for reducing the impact of natural disasters and for making better strategic decisions in the agricultural sector. Meinke and Stone (2005) highlighted numerous agricultural decisions that could be made given forecasts targeted to the intra-seasonal time scale. Reliable predictions for this extended range would help plan for key events such as the timing of the rainy season onset for planting decisions and rainy season cessation for harvesting decisions and provide early warning for the risk and potential timing of dry spells or damaging heavy rain for crop management and protection decisions.

The intra-seasonal time scale lies between daily weather and seasonal climate for which the MJO is considered to be a major source of predictability, especially in the tropics (Waliser, 2005; Wheeler *et al*., 2009). The MJO is a dominant mode of tropical variability on intra-seasonal time scales (Madden and Julian, 1971; 1972; 1994). The MJO's impact on rainfall has been widely documented (Donald *et al.*, 2006; Pohl and Camberlin, 2006; Wheeler *et al*., 2009; Zhang *et al*., 2009; Jia *et al*., 2010 and Berhane *et al*., 2015). Previous studies indicate that the onset of the South Asian monsoon is most likely to occur when the MJO convection just starts over the Indian Ocean (MJO phases 2 and 3), than in other phases (Zhang, 2013). About 50-80% of the total intra-seasonal variance in the Asian summer monsoon rainfall is related to the MJO (Zhang, 2013).

The real-time multivariate MJO (RMM) index developed by Wheeler and Hendon (2004) (WH04 hereafter) provides both real-time MJO information (position and strength) and a historical database. Using this index, much work has been done to study the effect of the MJO on rainfall variability over many parts of world (Wheeler *et al*., 2009; Zhang *et al*., 2009; Jia *et al*., 2010; Martin and Schumacher, 2011; Pai *et al*., 2011; Matthews *et al*., 2013 and Peatman *et al*., 2014).

The MJO influence on precipitation also extends to extreme events (Zhang, 2013). On a global scale, the occurrence of extreme rainfall events, defined as precipitation exceeding the 75^{th} percentile of the frequency distribution, is about 40% more frequent during active MJO periods than during its quiescent periods (Jones *et al*., 2004). Extreme rainfall, defined as precipitation exceeding the 75^{th} and 90^{th} percentile of the frequency distribution in the contiguous United States in boreal winter shows sensitivity to the MJO whereby the probability of occurrence of the extreme rainfall events is

twice as high when the MJO is active than inactive (Jones and Carvalho, 2012). Martin and Schumacher (2011) found that extreme rainfall with high rain rates was more frequently observed over the Caribbean during the MJO phases 1 and 2. The MJO impact on extreme rainfall leading to severe floods was studied by Zhu *et al*. (2003); Barlow *et al*. (2005); Aldrian (2008) and Tangang *et al*. (2008).

Even though the relationship between ENSO extremes and rainfall in SL has been well studied (Rasmussen and Carpenter, 1983; Suppiah and Yoshino, 1986; Ropelewski and Halpert, 1987; 1989; Suppiah, 1997; 1996; Kane, 1998; Sumathipala and Punyadeva, 1998; Punyawardena and Cherry, 1999; Malmgren *et al.*, 2003; Zubair and Repelewski, 2006), in regard to SL rainfall, however, little has been done to see the impact of the MJO on rainfall during all seasons in SL. Out of 4 climatic seasons, SIM is characterized by significant inter-annual and intra-seasonal variability. Previous studies identified ENSO and IOD seems to play a major role in the variability of the SIM rainfall on the sub-seasonal time scale. The SIM rainfall is enhanced (suppressed) by the EL Nino (La Nina) (Rasmussen and Carpenter, 1983; Suppiah, 1997; Zubair and Repelewski, 2006) and Positive (Negative) IOD (Chandimala and Zubair, 2007). However, there are only a few studies addressing the intra-seasonal characteristics of climatic seasons. Analyzing Global Precipitation Climatology Project (GPCP) rainfall data, Vialard *et al*. (2011) identified that the intra-seasonal rainfall anomalies over southern India and SL are significantly associated with the MJO from January to March. Given the location of SL near the heart of the MJO's convective envelope, SL is in a prime location to take advantage of recent advances in MJO prediction lead, being approximately three to four weeks at present (Gottschalck *et al*., 2010; Rashid *et al*., 2011; Zhang, 2013; Marshall *et al*., 2012; Neena *et al.*, 2014).

The main objective of this paper is to investigate the impact of the MJO on mean rainfall as well as on extreme rainfall events in SL for four climatic seasons such as FIM (15-March to 15-May), SWM (16-May to 15-September), SIM (16-September to 30 November) and NEM (1 December to 14 March). The corresponding large-scale lower tropospheric circulation and convective anomalies will also be analyzed to explain the impact of the MJO on the observed local rainfall.

Although the MJO exists all year-round, its strength undergoes a strong seasonal cycle, being strongest in boreal winter and weakest in boreal summer (Madden and Julian, 1994; WH04). Furthermore, the MJO shows a complex character with prominent northward propagation and variability extending much further from the equator

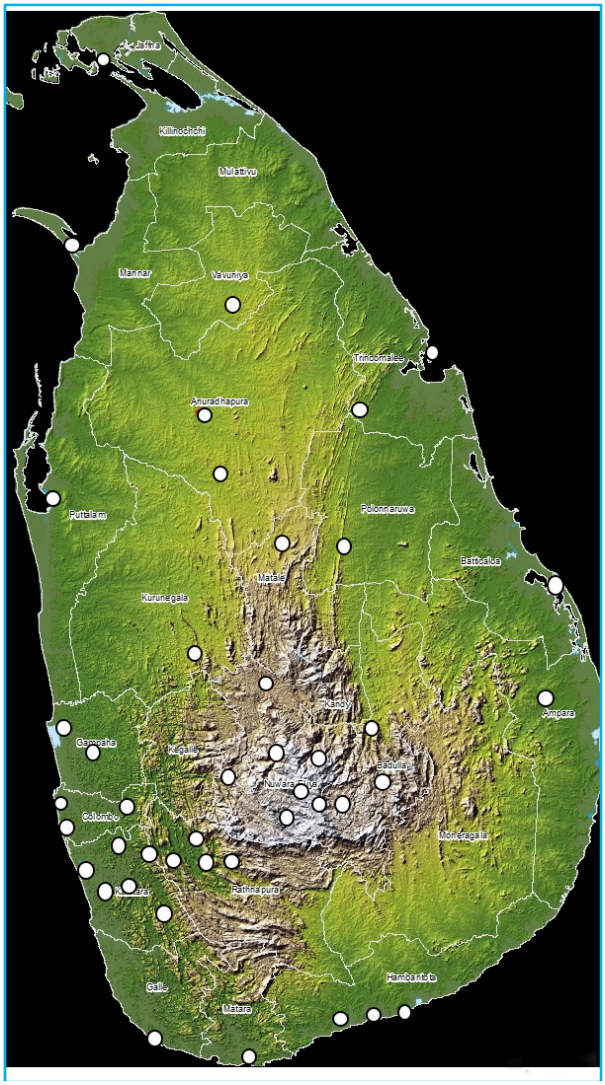

Fig. 1. Locations of 44 rainfall stations in Sri Lanka as used in this study

during boreal summer (Madden and Julian, 1994). Some studies indicate that the MJO cannot capture the northward propagating monsoon intra-seasonal oscillation completely (Lee *et al.*, 2013) during the Summer Monsoon season. Due to the near equatorial location, we assume that the MJO might be able to capture the intra-seasonal rainfall variability over SL during SWM season.

The remainder of the paper is organized as follows. Descriptions of the data and analysis method used are presented in section 2. In section 3, the variation of rainfall with respect to the MJO at different seasons & corresponding large-scale circulation and convective anomalies are investigated. Summary and discussion is presented in section 4 & conclusion is presented in section 5.

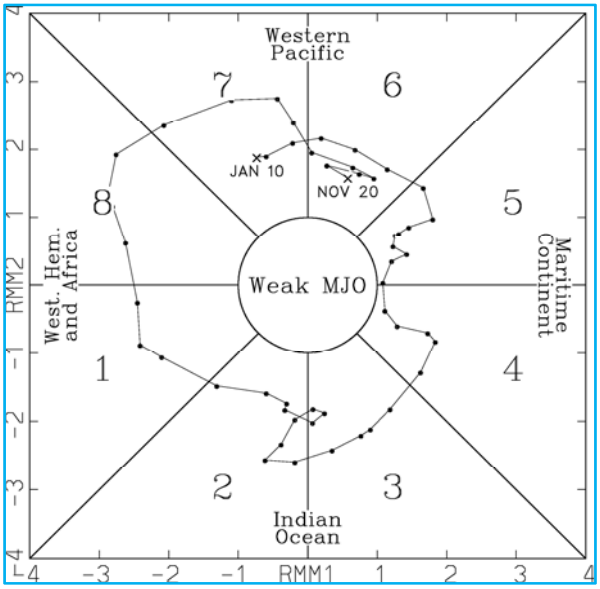

Fig. 2. Example phase diagram of RMM index (Wheeler and Hendon, 2004) for the period 20 November, 2007 to 10 January, 2008. Eight phases and corresponding approximate locations of enhanced convective signals of the MJO are labelled, *e.g.*, the "Indian Ocean" for phases 2 and 3. Points within the unit circle represent weak MJO

2. Data and methodology

2.1. *Rainfall data*

Daily rainfall data used were from 44 stations (Fig. 1) in SL covering the period from 1981-2010, collected, compiled and quality controlled by the Department of Meteorology, SL. Station rainfall data is used in this study because: (*i*) it is available for a long period, 1981-2010; (*ii*) it can highlight small spatial-scale variability better than some gridded satellite products and (*iii*) it can serve as a ground-truth to later work with high-resolution satellite-based products. Some of the data from these stations for the period 1981-2010 were missing. Out of 44 stations 60% of had less than 1.5% of days missing. Nearly 90% of stations had less than 5% of days missing. Stations located in the northern part of SL have more than 10% of days missing. Nearly 30% of daily rainfall data are not available at the Jaffna meteorological station, owing to frequent disruptions caused by civil unrests there. Due to the limited and sparsely distributed stations in the northern and eastern part of the country, Climate Hazards Group Infra-Red Precipitation with Station data (CHIRPS; Funk *et al.*, 2015) from 1981-2010 were also analysed and composite maps based on CHIRPS data indicate similar results (not shown). However, we also note that satellite-based rainfall products such as CHIRPS have their own problems, especially in mountainous terrain and around coasts (Rauniyar *et al.*, 2017), so the results from both rainfall products require careful interpretation. While comparing with 30 year averages (1981-2010) of station data [Fig. 3(e)] with CHIRPS data [Fig. 3(f)], it is evident that CHIRPS data under estimate the orographic rain [Figs. 3(f&g)] in Sri Lanka.

2.2. *MJO index*

The Real-time Multivariate MJO (RMM) index developed by WH04 defines the MJO through projection of daily anomaly data onto the leading pair of empirical orthogonal functions (EOFs) of the combined fields of equatorially-averaged (15° S-15° N) Outgoing Longwave Radiation (OLR), 850 hPa zonal wind and 200 hPa zonal wind, to obtain two principal component time series (called RMM1 and RMM2). The RMM1 and RMM2 indices define a 2D phase space. This phase space is used to define eight "strong" MJO phases, each corresponding to the geographical position of its active convective center (labeled 1-8 in Fig. 2) and a "weak MJO" category defined when the amplitude is less than 1 (within the circle representing weak MJO, Fig. 2). These phases make up a full MJO cycle originating from the western Indian Ocean and decaying over the central Pacific. For instance, phases 2 and 3 mark the time when the MJO's convective envelope is centered over the western and eastern Indian Ocean and phases 6 and 7 over the western Pacific.

2.3. *Observed and re-analysis data*

Observed Outgoing Longwave Radiation (OLR) data from the National Oceanic and Atmospheric Administration (NOAA) polar-orbiting satellites are used as a proxy for deep tropical convection. Interpolation is applied separately to the "day" and "night" maps to remove missing data and these maps are then averaged to provide a single daily map on a 2.5° grid as described by Liebmann and Smith (1996).

Zonal (u) and meridional (v) winds at 850 hPa level from 1981 to 2010 are obtained from the National Centers for Environmental Prediction-National Center for Atmospheric Research (NCEP-NCAR) re-analysis (Kalnay *et al.*, 1996) on a 2.5° grid to create composite maps of circulation.

2.4. *Composite analysis*

Composites of rainfall and circulation are computed for each of the eight phases of the MJO and separately during each season (SWM, NEM, FIM, SIM) using data for the 30 years from 1981-2010. Following WH04, the MJO is conveniently divided into eight phases, with each phase lasting an average of about 6 days. Here we use

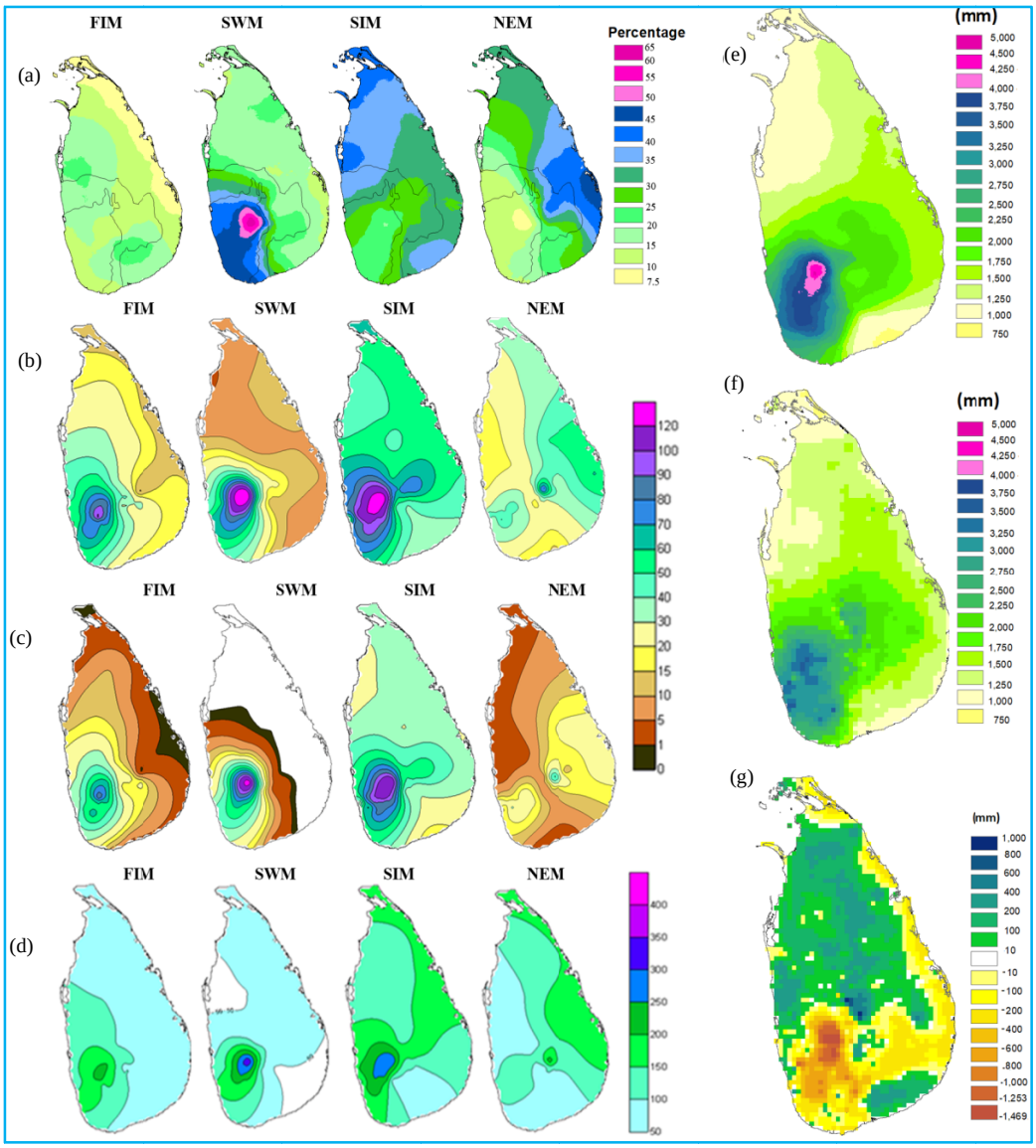

Figs. 3(a-g). (a) Contribution of Seasonal rainfall to annual rainfall as a percentage (%) for four climate seasons, (b) Weekly mean rainfall (mm) for four climate seasons, (c) Weekly median rainfall (mm) for four climate seasons, (d) Threshold for 90th percentile of weekly rainfall (mm) for four climate seasons, (e) Annual average of rainfall (mm) from station data (1981-2010), (f) Annual average of rainfall (mm) from CHIRPS data (1981-2010) and (g) Difference of Annual average rainfall (mm) between CHIRPS and station rainfall

7-day running mean (overlapping weekly) rainfall data for rainfall composite analysis. For the overlapping weekly data, we formed composites using the MJO category occurring on the middle day, providing the best estimate of the contemporaneous relationship. Subtracting the mean value at each phase at a particular station from the climatological mean of that station for each season produces the composite anomalies.

The MJO being a major source of global predictability on the sub-seasonal time scale (Waliser, 2005), probability composites provide useful information for extended range forecasting. Probability composites for rainfall are generated with total rainfall data R (t) by counting the number of days at each station for each composite phase for which R is greater than a predefined rainfall threshold T and then dividing by the total number of days in that composite phase to form a probability. The threshold T can be a function of the station and the season. Here we show results using T set to the median and highest decile (*i.e.*, the 90th percentile) of weekly rainfall at each station.

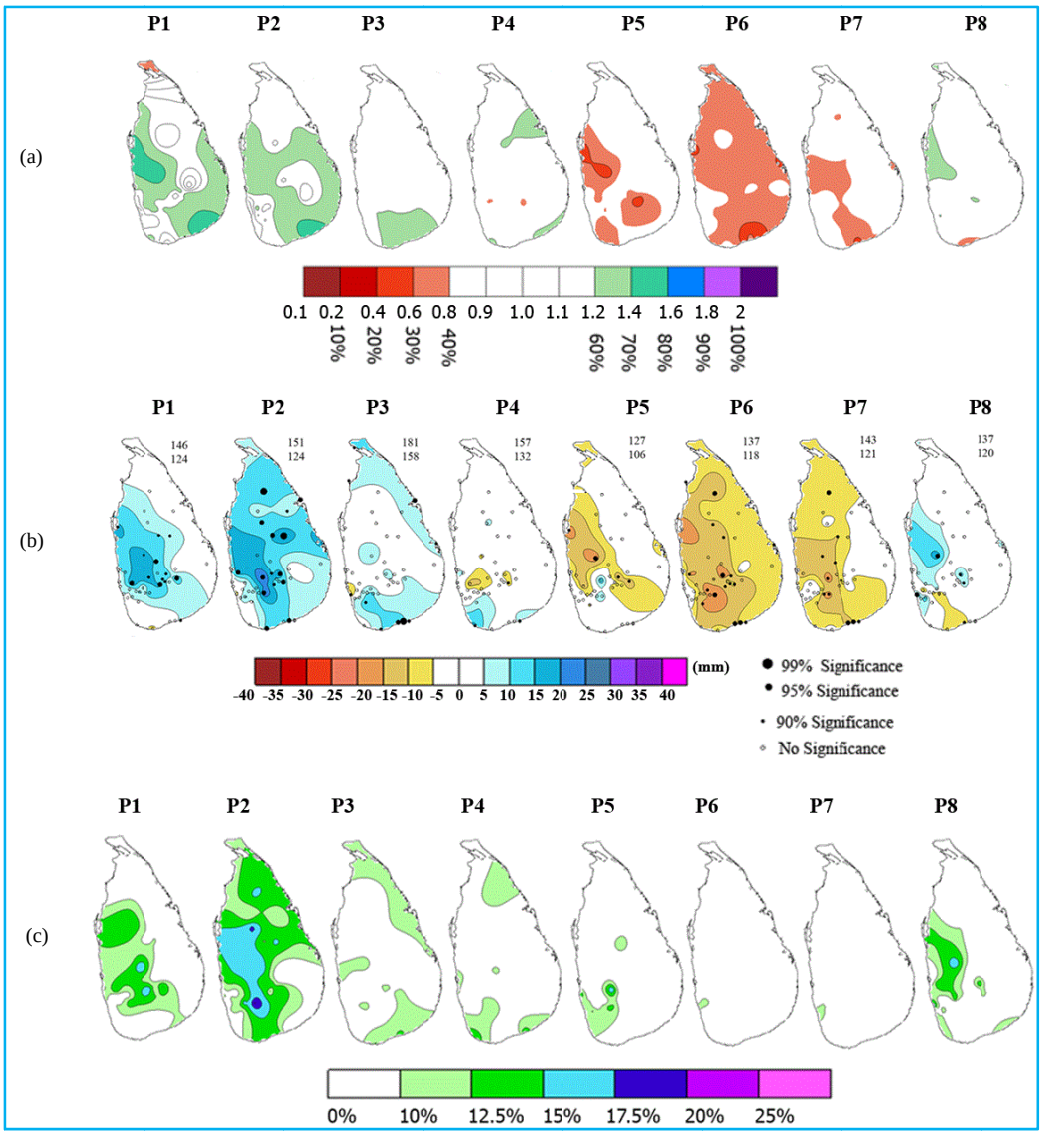

Figs. 4(a-c). MJO composites of weekly rainfall probabilities. (a) [Rainfall probabilities refer to the chance of weekly rainfall exceeding the median, expressed as a ratio with the mean probability], Composite Maps of weekly rainfall anomaly, (b) [Black large, medium and small solid circles denote the stations that pass the 99%, 95% and 90% significance tests, respectively, based on the Student's *t* test. Open circles indicate the stations with no significance. The maximum and minimum numbers of recorded days in each phase at the 44 stations are given in the upper-right corner of each phase], composites of weekly rainfall probabilities, weekly rainfall exceeding the 90th percentile and (c) for FIM season for phases 1-8

Statistical significance for the composites was judged using a local *t*-test applied to the difference between two sample means. For each MJO phase, the null hypothesis of the field test is that there are no significant differences between the composite anomalous field and zero (Shiryaev, 1996).

Compared with daily rainfall data, 7-day running mean rainfall data is less skewed with an approximate normal distribution allowing the *t*-test to be used. The composites were estimated to be significantly different from zero at the 95% confidence level. The formula is :

$$t = \frac{\left|\sum_{i=1}^{N} \frac{F'}{N}\right|}{\sigma\sqrt{1/N'}}$$

where, $\sum \frac{F'}{N} \sum \frac{F'}{N}$ is the anomaly field composite for different MJO phase categories, F' is the daily anomaly

field for different MJO phase categories, σ is the daily standard deviation of the particular season and N' is the effective sample size approximation by $N' \cong N\frac{1-\rho}{1+\rho}\frac{1-\rho}{1+\rho}$ (Wilks, 2006), *N* is the number of days in each MJO phase andρ is the lag-1 autocorrelation coefficient of particular season (Jia *et al*., 2010).

3. Results

The analysis of MJO-related variations of rainfall and circulation is performed and described separately for the seasons SWM, FIM, SIM and NEM, as defined above. For each of these seasons over the analysis period (1 January, 1981 to 31 December, 2010) of this study, the number of days under each of the 8 strong MJO phases is given in Table 1. For example, there are 146 days in the MJO phase 1 during the FIM season for the 1981-2010 period. The number of days under each of the MJO phases is slightly different for some stations due to missing data [the maximum and minimum numbers in each panel of Figs. 4(b), 6(b), 8(b), 10(b)].

3.1. *FIM season*

Looking first at the mean rainfall of the FIM season [Fig. 3(b)], the southwestern quarter receives over 30 mm of weekly mean rainfall with the peak greater than 60 mm per week over the western slope of the central highlands. Most other parts have weekly mean rainfall around 10-30 mm. During the Inter-monsoon seasons (*i.e*., both FIM and SIM) most convective activity is associated with the formation of mesoscale circulations due to differential heating caused by horizontal variations in land surface characteristics.

Figs. 4(a&b) show the composite maps of probability of receiving above median weekly rainfall and weekly rainfall anomaly respectively for the 8 different categories of the MJO during FIM. There is a higher chance of occurrence of above median rainfall over northwest and southeast quarters during phases 1 and 2 [Fig. 4(a)]. Similarly, the rainfall anomalies are slightly positive over western parts, except southwestern coastal region during phase 1 and the anomalies are positive over most parts of SL during phase 2 [Fig. 4(b)].

Fig. 5 reveals the low-level circulation pattern and large-scale convective activity associated with the MJO by the negative OLR anomaly. Note that this and later OLR composites are for slightly different seasons to those displayed in Wheeler and Hendon (2004), but our detailed comparisons show that they are consistent. During phase 2, the large-scale MJO envelope with negative OLR anomaly is located over SL. The positive rainfall anomaly

TABLE 1

The number of days under each of the 8 strong MJO Phases (RMM ≥ 1) and weak MJO Phases (RMM<1) during the 30 SWM, FIM and SIM seasons and 29 NEM seasons from 1981 to 2010

MJO Phase	FIM	SWM	SIM	NEM
1	146	375	173	183
2	151	314	196	240
3	181	176	151	295
4	157	199	179	245
5	127	283	223	229
6	138	291	193	240
7	143	229	133	309
8	137	240	150	251
Weak MJO	680	1583	882	1031

pattern all over the island [Fig. 4(b)] with higher probability of receiving above median rainfall over the north western and south eastern parts in phase 2 [Fig. 4(a)], appears to be a direct influence of the MJO envelope. Noticeable changes in the strength of the positive rainfall anomalies are also evident in the eastern parts [Fig. 4(b)] due to easterly wind anomaly present in phase 2 (Fig. 5).

Probability composites suggest that rainy activity is confined to the southern part of the country in phase 3 [Fig. 4(a)], but anomaly composites indicate slightly positive rainfall anomaly over the north and north eastern parts in phase 3 [Fig. 4(b)]. During phase 3, the MJO envelope with negative OLR anomaly is still located in the Indian Ocean but the convective core has moved to south of SL. During phase 4 neutral conditions appear over most parts of the island. Then, reduced rainfall activity is evident from phases 5 to 7 with widespread suppressed rainfall activity in phase 6. Large-scale suppressed convective activity with positive OLR anomalies is apparent over SL during phases 6 and 7 [Fig. 5). Anomalous anticyclonic circulation also appears in the southwest Bay of Bengal (BoB) in phase 7. With the eastward movement of suppressed MJO activity into Maritime continent in phase 8, slightly above normal rainfall is evident over west northwest parts of the island [Fig. 4(b)]. As there is no predominant wind flow over SL, variable light winds prevail during the FIM season in the absence of large-scale external forcing. The effect of land-sea breeze circulation is prominent along the coastal regions. This may be linked to coastal convergence with lower tropospheric anomalous easterly winds [Fig. 5] in phase 8.

In this study extreme events are defined as 7-day running mean (over lapping weekly) rainfall exceeding the

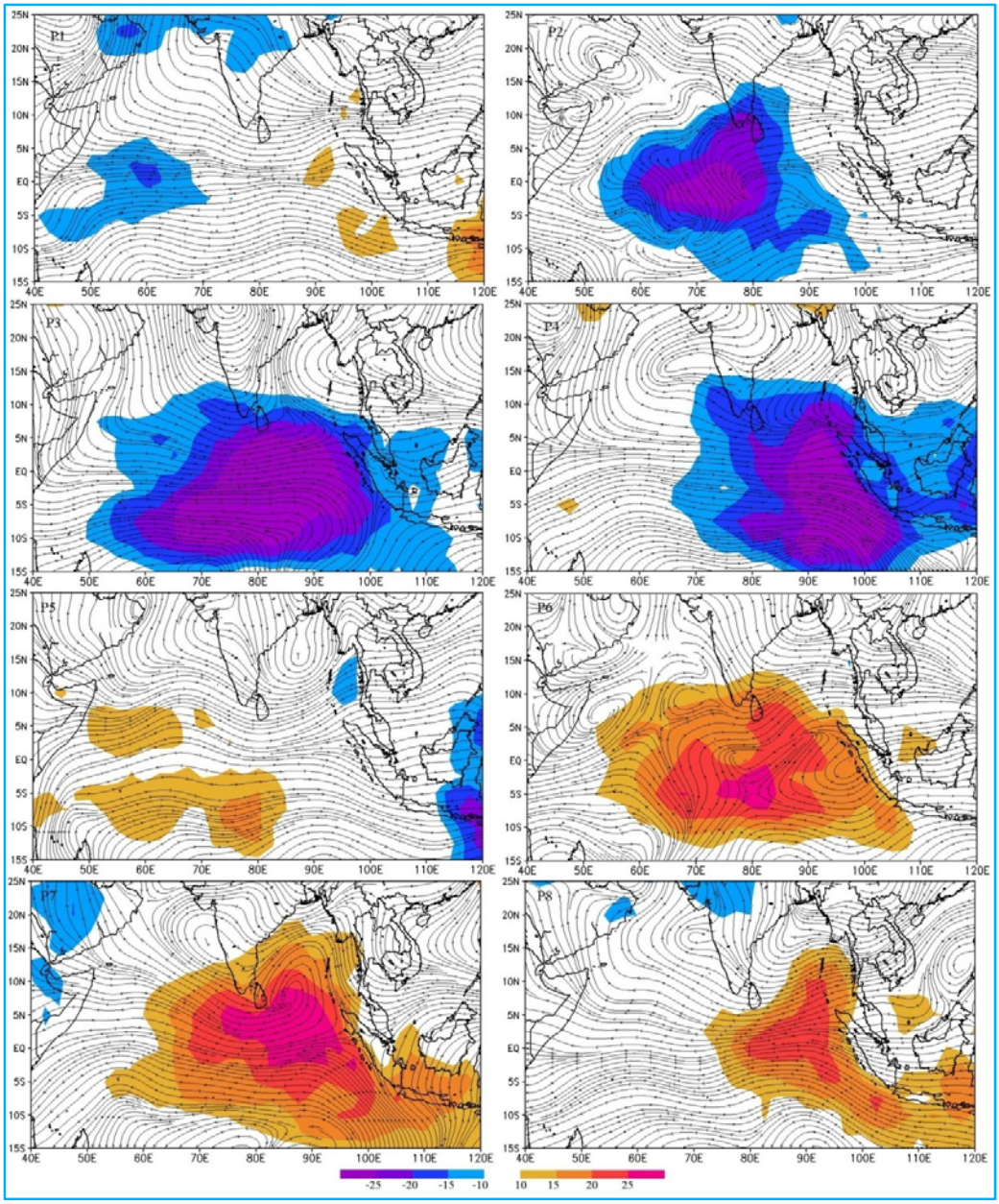

Fig. 5. Composite OLR (shaded) & 850-hPa wind (streamlines) anomalies for MJO phases during FIM (Region : 25° N-15° S, 40° E-120° E)

90th percentile. As the extreme events defined for the 95% threshold (not shown) indicate that the phases and spatial patterns of the MJO impact is quite similar to the impact on the 90% threshold [Fig. 3(d)], we assume that the 90% threshold might be able to capture the MJO influence on extreme rainfall events in SL.

Fig. 4(c) represents MJO composites of weekly rainfall probabilities, weekly rainfall exceeding the 90th percentile (shading) for FIM seasons for phases 1-8. Higher chance of occurrence of extreme precipitation events during FIM season can be seen during phase 2 compared with the other MJO phases [Fig. 4(c)].

3.2. *SWM season*

During the SWM season, the western slopes of central highlands receive over 120 mm weekly mean rainfall and the southwestern coastal belt around 50-70 mm [Fig. 3(b)]. The intra-seasonal variation of SWM

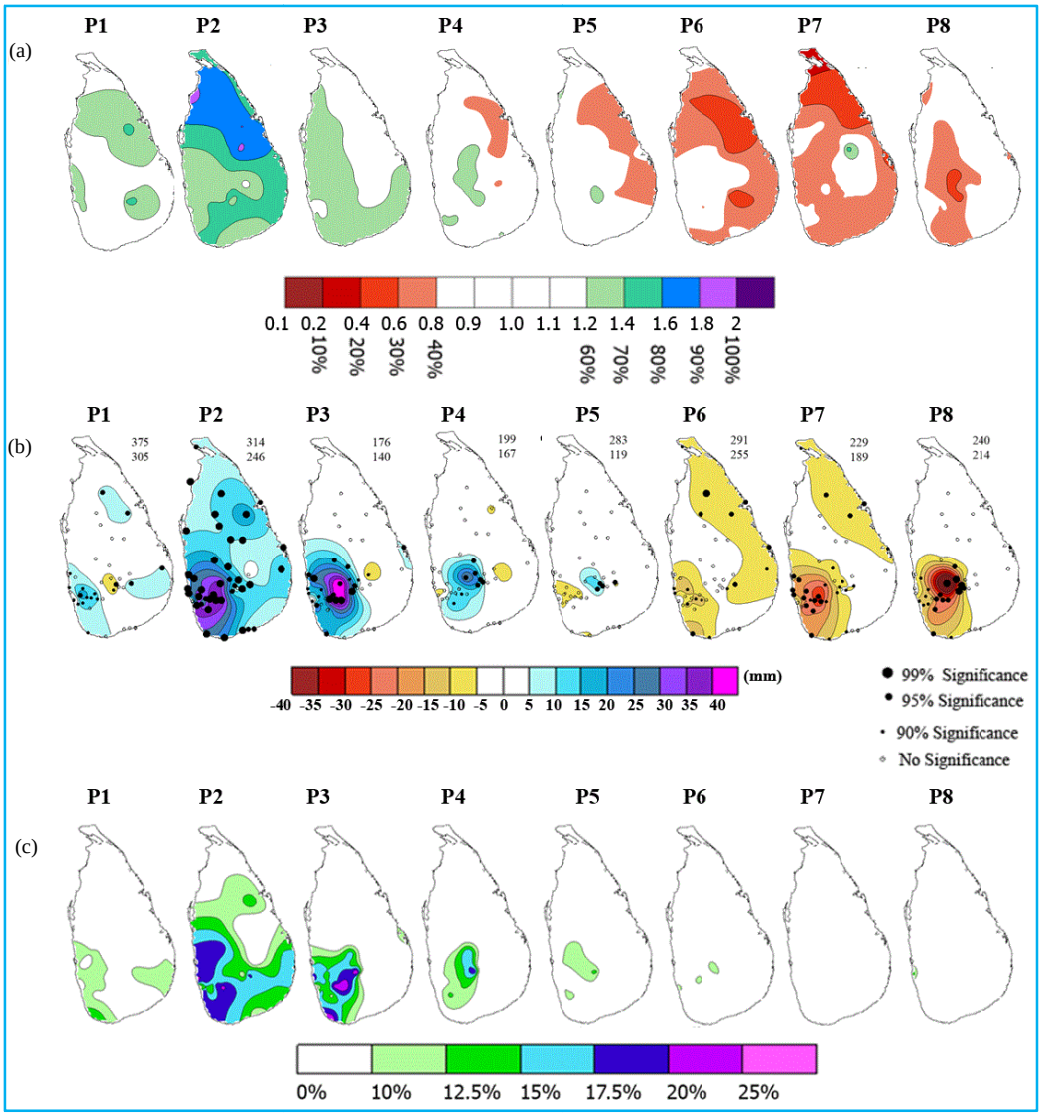

Figs. 6(a-c). As in Fig. 4, but for the SWM

rainfall distribution over SL associated with various phases of eastward propagating MJO life cycle is examined to understand the mechanism linking the MJO to the intra-seasonal rainfall variability in SWM.

During phase 1, isolated patches of above normal rainfall anomalies are evident in the western, north eastern and south eastern parts of SL [Fig. 6(b)]. Composites probability maps also reveal the same spatial pattern during phase 1 [Fig. 6(a)]. Large-scale circulation pattern reveals an anomalous easterly winds over SL that weakens the southwest monsoon wind flow (Fig. 7). Coastal convergence may play a role in above normal rainfall anomaly in the southwest parts in phase 1. During phase 2, widespread positive rainfall anomalies can be seen all over the country, with enhanced rainfall anomalies over the western slopes of central hills [Fig. 6(b)]. Most importantly, the majority of stations located in the north eastern, eastern and north western parts (dry zone) receive positive rainfall anomalies exceeding 100% relative to the climatological seasonal mean in phase 2. The MJO envelope with convective core, located in the vicinity of SL and anomalous cyclonic circulation located to the southwest of SL, together are responsible for the positive rainfall over SL in phase 2 (Fig. 7). In general, the dry zone (*i.e.*, the northern and eastern parts of SL) where the seasonal median drops to 0 mm week^{-1} [Fig. 3(c)] receives less rainfall during SWM season. During phase 1, there is a higher probability of increasing rainfall activity over the dry zone. Enhanced probability of rainfall exceeding the

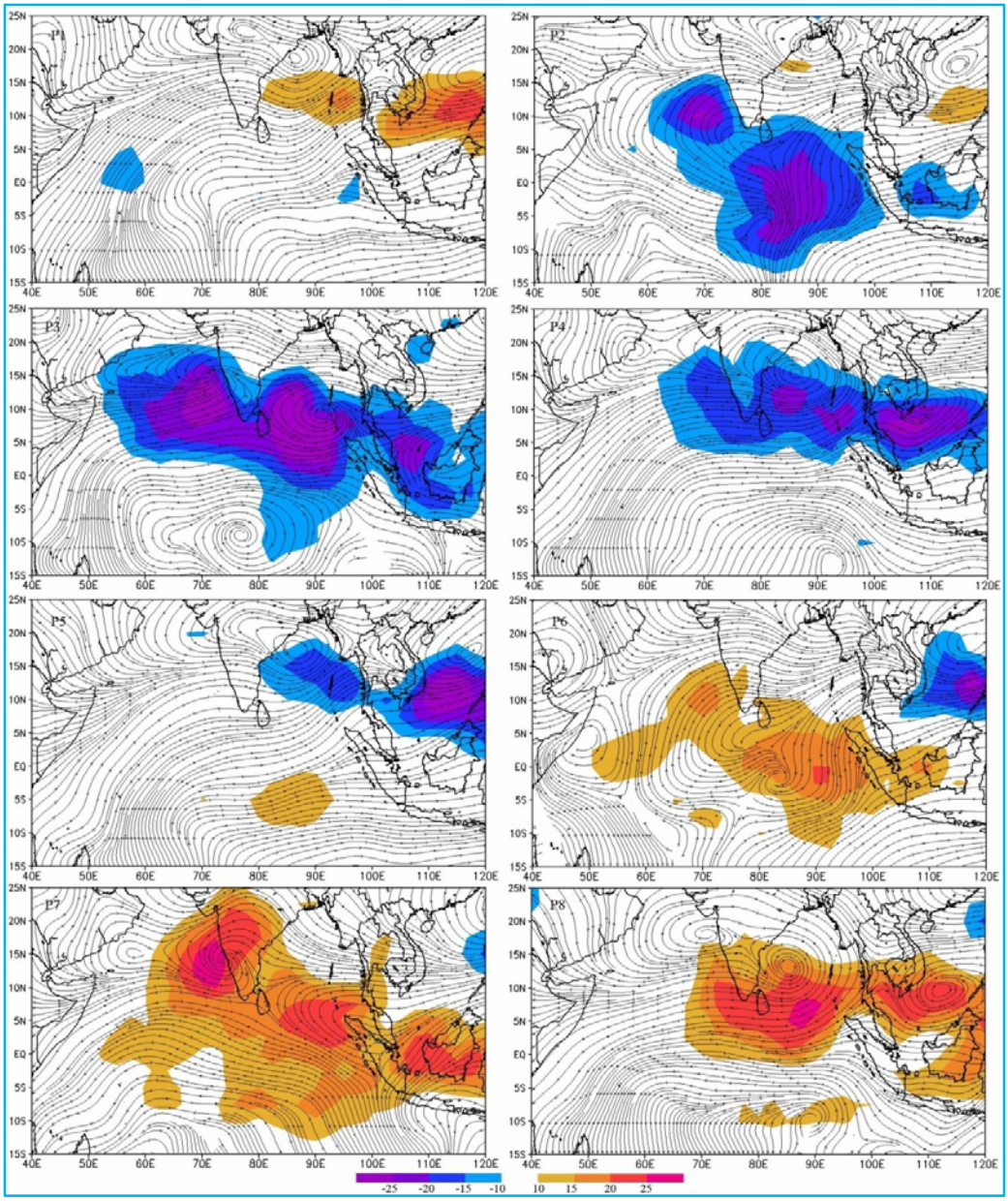

Fig. 7. As in Fig. 5, but for the SWM

median is evident all over the country in phase 2 with a greater chance (more than 80%) of receiving rainfall over the dry zone [Fig. 6(a)].

Higher probability of receiving wet conditions over the western and southern parts including the western slopes of the central hills is obvious in phase 3 [Fig. 6(a)] with anomalous westerly flow feeding into an anomalous cyclonic circulation centered in southwest BoB (Fig. 7), enhancing the monsoonal flow bringing above normal rainfall anomalies over the south western part of the country [Fig. 6(b)]. In phase 4, the rainfall anomaly pattern was similar to that of phase 3, with a further northward movement of anomalous vortex over BoB that strengthens the monsoonal flow across SL. Anomalous westerly flow still persists in phase 5 but the anomalous cyclonic circulation center moves further northward. Western slopes of the central hills receive slightly above normal rainfall, but the western coastal areas receive below normal rainfall in phase 5. Phases 6, 7 and 8 are associated with the dry signal over SL. A dry condition over the north eastern parts of SL is evident from

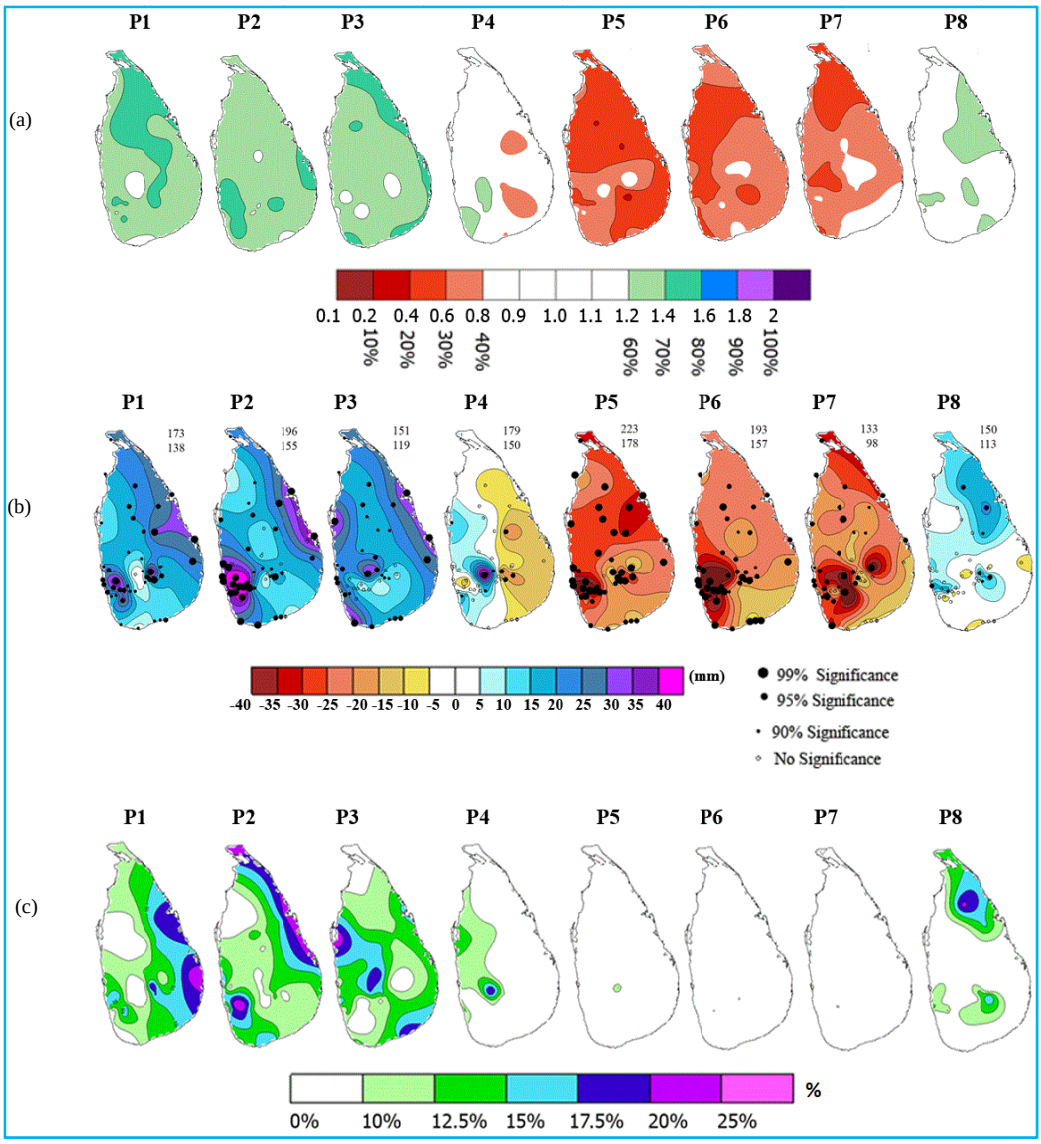

Figs. 8(a-c). As in Fig. 4, but for the SIM

phases 4 to 6 with gradual expansion of the area of reduced rainfall activity [Fig. 6(a)]. A widespread dry condition is evident in phase 7. Reduction of rainfall activity over western slopes of central hills is obvious in phase 8 [Fig. 6(b)]. Anomalous anti-cyclonic circulation is evident over the vicinity of SL during phases 6 to 8 (Fig. 7).

There is a higher chance of occurrence of extreme rainfall events over low-lying areas in the southwest part which is vulnerable to floods in phases 2 and 3 and the western slopes of central hills vulnerable to landslides during phase 3 [Fig. 6(c)].

3.3. *SIM season*

The SIM season shows the uniform distribution of rainfall over SL. Almost the entire island receives in excess of 40 mm of weekly mean rain during this season, with the southwestern slopes receiving high weekly mean rainfall in the range 75 mm to 120 mm [Fig. 3(b)]. There is a prominent increase of rainfall due to the overhead position of the ITCZ as it moves southward movement (Suppiah, 1996). The influence of depressions is common during SIM (Malmgren *et al.*, 2003), when the whole country experiences strong winds with widespread rains, sometimes leading to floods and landslides.

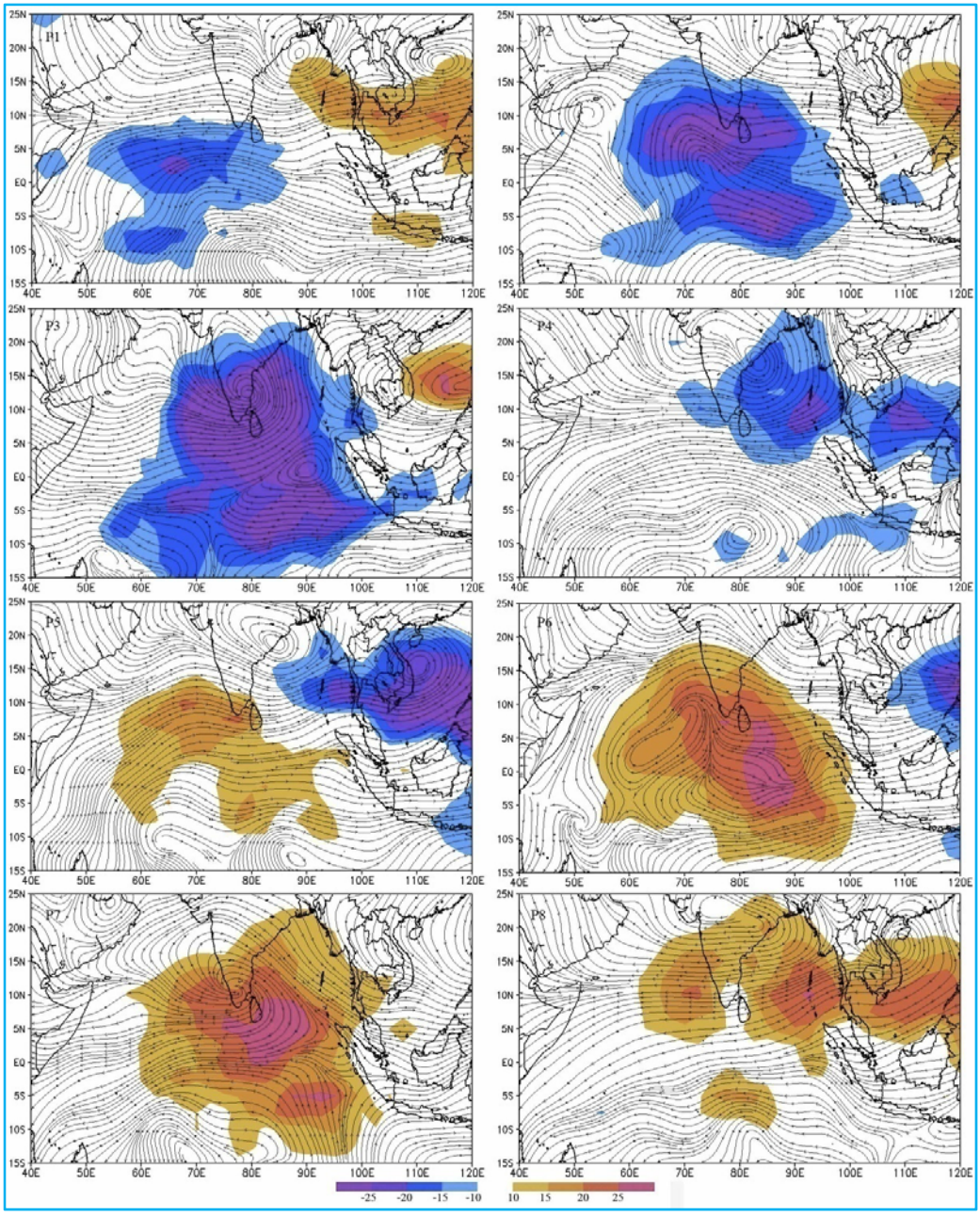

Fig. 9. As in Fig. 5, but for the SIM

It is clearly evident that during the MJO's life cycle, the strongest signal can be seen during SIM, the transition period from SWM to NEM [Figs. 8(a&b)]. It is obvious that widespread wet conditions prevail during phases 1 to 3 while widespread reduced rainfall activity prevails during phases 5 to 7. The transition from widespread wet conditions to dry conditions can be seen in phase 4 and conversely in phase 8.

There is enhanced probability of rainfall activity over the entire country from phases 1 to 3 with a 70% chance of receiving above median rainfall over the north eastern parts in phase 1, over the south western and eastern parts (such as Ampara and Batticoloa districts) in phase 2 and along the north eastern, eastern and south eastern coastal belt in phase 3 [Fig. 8(a)].

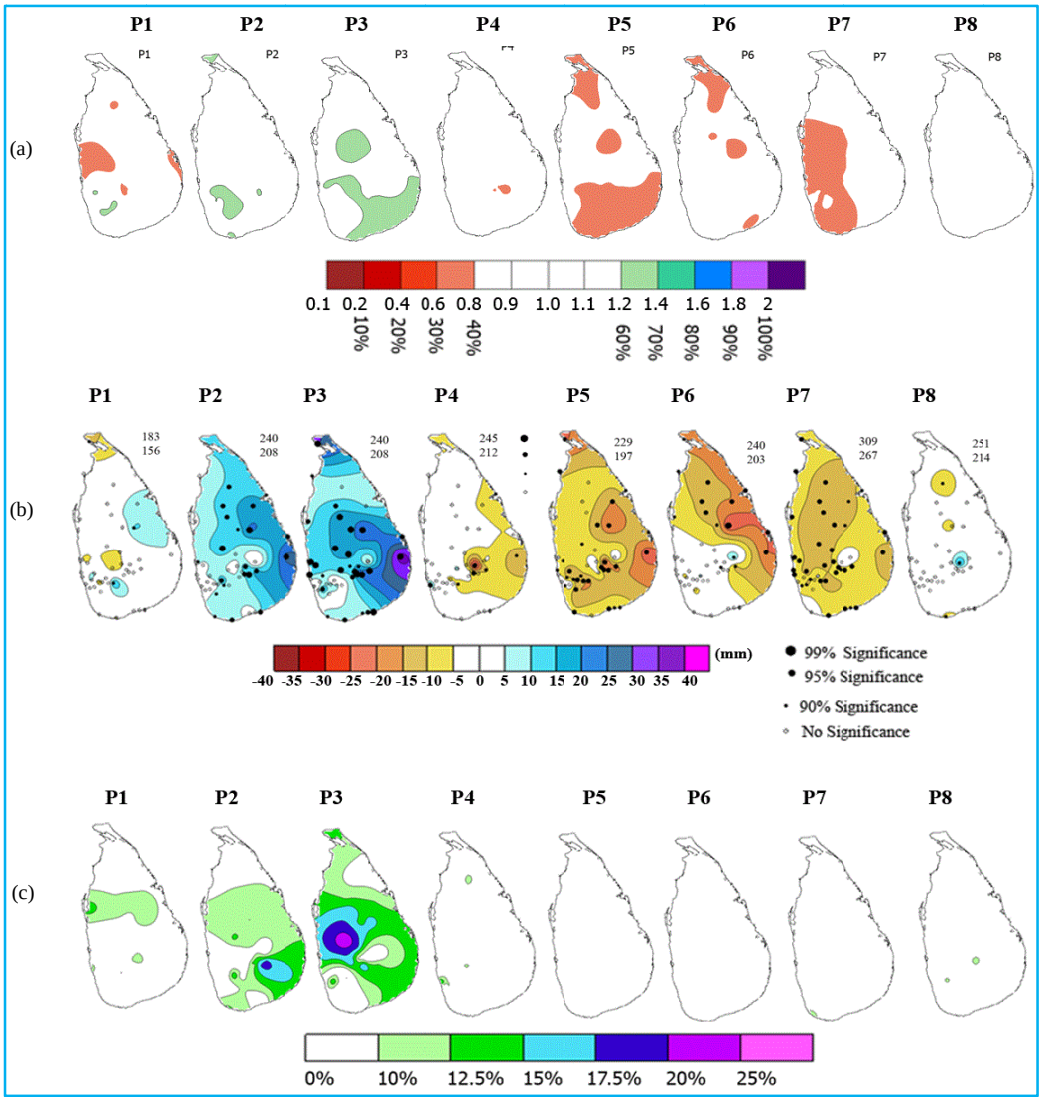

Figs. 10(a-c). As in Fig. 4, but for the NEM

During the suppressed rain activity which is evident from phases 5 to 7, the probability drops to below 30% over the northern, north eastern and south eastern parts in phase 5, northwestern parts in phase 6 and over northern parts in phase 7 [Fig. 8(a)]. The transition from wet to dry conditions is evident in phase 4 with higher probability of rainfall over western parts and suppressed rainfall with lower probabilities over eastern parts [Fig. 8(a)] and dry to wet conditions is apparent in phase 8 with enhanced probability of rainfall over northeastern parts.

Convective core with negative OLR anomalies are evident to the west of SL in phases 1 and directly over SL in phases 2 and 3 (Fig. 9). Large-scale circulation pattern reveals an anomalous easterly winds over SL in phase 1 (Fig. 9) resulting above normal rainfall [Fig. 8(b)] in the eastern parts of the country. Coastal convergence may contribute to above normal rainfall anomaly in the western parts in phase 1 [Fig. 8(b)].

Enhanced likelihood of rainfall during phases 2 and 3 [Figs. 8(a&b)], occurs in conjunction with anomalous trough to the west of SL and cyclonic circulation to the northwest of SL respectively (Fig. 9).

Suppressed convection with positive OLR anomalies are evident to the west of SL in phases 5 and directly over SL in phases 6 and 7. Suppressed rainfall in phases 6 to 7 [Figs. 8(a&b)] occurs in conjunction with anomalous divergence to the west of SL and anti-cyclonic circulation to the northwest of SL respectively (Fig. 9).

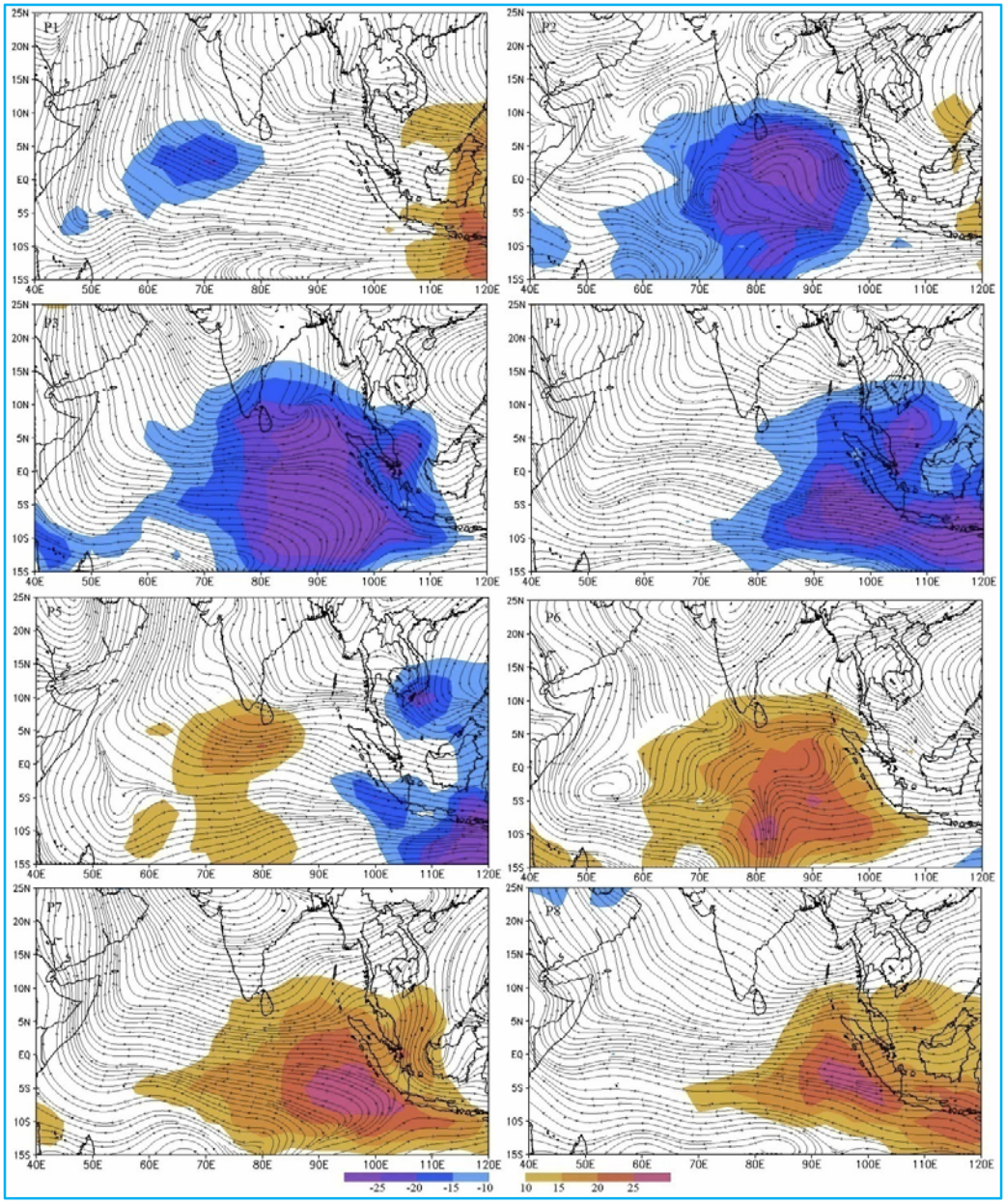

Fig. 11. As in Fig. 5, but for the NEM

As there is no predominant wind flow across the country during this season, anomalous westerlies in phase 4 and anomalous easterlies in phase 8 brings enhanced rainfall to the western parts and eastern parts of the country, respectively [Figs. 8(a&b) and Fig. 9].

During SIM, the entire country experiences long spells of widespread rains, sometimes leading to floods and landslides. Low lying areas in the north eastern parts have a higher chance of the occurrence of extreme rainfall events during phases 1, 2 and 8 that may lead to floods [Fig. 8(c)]. During phase 2, there is an enhanced probability of receiving heavy rainfall in landslide and flood prone areas in the southwest quarter [Fig. 8(c)]. There is a higher chance of occurrence of extreme rainfall events over the northwestern and southeastern parts during phase 3. Even though convective activities play an important role during the FIM and SIM seasons, the influence from large scale external forcing associated with the MJO is more prominent during SIM than FIM as indicated by the higher/lower probabilities of rainfall exceeding the median [Fig. 8(a) compared to Fig. 4(a)].

3.4. *NEM season*

During NEM season, moist wind blowing from BoB produces seasonal rainfall in the eastern parts of the country [Fig. 3(b)]. Highest rainfall figures are recorded in north- eastern slopes of the hill country and eastern slopes of the Knuckles/Rangala range. Westward propagating high frequency equatorial waves such as easterly waves and equatorial Rossby waves play an important role in the enhancement of rain activity over SL during NEM (IMD, 1973). On the other hand, cool dry weather can be experienced over many parts of the country, when northerly to northeasterly winds blows from the high-pressure centers located over the Indian landmass (www.meteo.gov.lk).

The NEM is the season when the rainfall variability is less affected by the MJO. There is a higher probability of increasing rainfall activity over the interior parts of the southwest quarter, southeastern parts and northern part during phase 2 and over southeastern parts and northwestern parts in phase 3 [Fig. 10(a)]. The rainfall anomalies are positive over the entire SL with evidence of enhancement of wet conditions in phases 2 and 3 [Fig. 10(b)]. Suppressed rainfall is evident over southeastern parts, northern and northeastern parts in phases 5 and 6 and southwestern parts in phase 7. Signal is weak during phases 1, 4, 8 [Figs. 10(a&b)].

The anomalous easterly winds over SL in phase 1 have strengthened the NEM flow resulting in above normal rainfall anomalies over the eastern part of SL (Fig. 11). The MJO envelope with convective core is located to the south and southeast of SL in phases 2 and 3 respectively (Fig. 11). Convergence of anomalous easterly winds over SL in phase 2 (Fig. 11) and anomalous cyclonic circulation pattern in the southwest BoB in phase 3 (Fig. 11) enhances the rainfall activity over most parts of the country in phases 2 and 3 [Fig. 10(b)]. The dry conditions with negative rainfall anomalies can be seen from phases 4 to 7 especially over the northeastern parts. In phase 8, weakening negative anomalies over most of the island are evident.

There is a higher chance of occurrence of extreme rainfall events over eastern slopes of central hills, vulnerable to landslides in phase 2 and over low lying areas vulnerable to flood in southeastern coastal areas in phases 2 & 3 and northwestern parts in phase 3 [Fig. 10(c)].

The large-scale OLR anomaly pattern shows that the negative OLR anomalies associated with enhanced convection and positive OLR anomalies associated with subsidence areas have moved south of equator during NEM (Fig. 11).

The southward shift of the MJO envelope with convective core away from the equator during NEM, slightly reduces the impact of the MJO on NEM rainfall especially in the composites of probability of receiving above median rainfall [Fig. 10(a)]. Conversely, widespread positive rainfall anomalies in phases 2 and 3 that are not clearly evident in probability composite maps indicate that the occurrence of extreme rainfall events may notably influence the rainfall anomaly in NEM [Fig. 10(b)].

4. Discussion

It is identified that the greatest impact of the MJO on SL occurs during the SIM season. The economic importance of intra-seasonal rainfall variations in SIM is considerable because the major agricultural season called “Maha” starts with the onset of SIM. Nearly 72% of paddy rice, which is one of the principle crops of SL, is grown during the Maha season (September to March) in dry areas, where water resources are stressed (De Silva *et al.*, 2007). Both deficient and excess rainfall conditions have been found to significantly contribute to the reduction of rice yields (Yoshino and Suppiah, 1983). There is also variability in the sowing dates and duration of cultivation within the island (Yoshino and Suppiah, 1983). Therefore, it seems likely that better rice production planning decisions could be made with the information contained in this paper.

Influence of the MJO on SWM seasonal rainfall is also significant. Long lasting monsoon rain may result in floods in the low-lying areas and landslides in hilly areas. Rains can be experienced at any time during the day and night. Changing patterns of SWM rainfall as well as the frequency of the occurrence of extreme events often cause severe floods or droughts and greatly impact people’s daily lives, the development of economy and agriculture. For instance, SL’s power generation is highly dependent on hydropower facilities and most of the hydropower reservoirs are located along the western slopes of the central hills that receive substantial amount of rainfall during SWM. Hence, Intra-seasonal rainfall variability in SWM would have a significant impact on hydropower generation of SL.

Convection during the FIM period is often isolated and localized predominately over land, generally initiated by sea breezes and other local circulations and orography (Suppiah and Yashino, 1984). Scale interaction of rainfall and its modulation by intra-seasonal scale phenomena (Ichikawa and Yasunari, 2008) may also play an important role during FIM. According to Slingo *et al.* (2003), scale interaction is defined as the process that describes the influence of the large-scale and low-frequency variability on small spatial scale high-frequency variability of the

climate system and vice versa. The MJO is considered to be large spatial scale low-frequency variability, whereas mesoscale convective phenomena are small in spatial scale and have a high frequency. The large-scale MJO envelope of precipitation is comprised of many smaller mesoscale weather systems (Nakazawa, 1988), embedded in individual cumulonimbus elements. The large-scale conditions in the MJO provide the environment to develop small-scale convective clouds (Zhang, 2005).

Previous studies have emphasized the pronounced seasonal variation of the MJO activity, with strongest activity shifting south of the equator in late boreal winter (Salby and Hendon, 1994; Zhang and Dong, 2004).With the southward shift of the MJO envelope during boreal winter (Salby and Hendon, 1994; Zhang and Dong, 2004; Zhang, 2005), direct impact of the MJO is slightly reduced during the NEM season.

5. Conclusions

The impact of the MJO on intra-seasonal rainfall variability in SL is examined using 30 years of data from 1981-2010. Composites of weekly rainfall anomalies, probability of receiving above the median weekly rainfall and probability of receiving above the highest decile weekly rainfall are constructed for each of the eight strong MJO phases. Real-time multivariate MJO index (WH04) and daily rainfall data from 44 stations are used over SL for four climatic seasons, namely SWM from mid-May to mid-September, NEM from December to mid-March and the transition periods between two monsoon seasons called FIM and SIM seasons.

Considering all four seasons, SL rainfall appears to be directly influenced by the MJO's tropical convective signal with the largest positive anomalies in phases 2 and 3 when the MJO convective envelope is located over the Indian Ocean and largest negative anomalies in phases 6 and 7 when the MJO convective envelope is located over the western Pacific. Of the four seasons, the greatest impact occurs during SIM with well-marked wet signals in phases 1 to 3 and dry signals in phases 5 to 7, respectively. The MJO's impact on SL rainfall during SWM is also significant with wet signals in phases 2 to 4 and dry signals in phases 6 to 8. A relatively smaller MJO influence is found in the other two seasons (FIM and NEM) with wet signals in phases 2 and 3 and dry signals in phases 5, 6 and 7.

Composites of lower tropospheric wind and convective anomaly are also investigated in order to examine how the rainfall anomalies are associated with large-scale low-level circulations. It is obvious that low-level circulation anomalies play a major role in enhancement and suppression of rainfall activity during different phases of the MJO in all seasons. Anomalous vortices in the vicinity of SL aid in the production of widespread rainfall over the island. Westerly anomalies associated with anomalous vortices in BoB during phases 3 to 4 in SWM season enhance SWM flow producing copious rainfall over southwest quarter especially over the western slopes of the central hills. Similarly, easterly anomalies connected with the anti-cyclonic circulations in the BoB in phases 6 to 8 during SWM season weaken the monsoonal flow, bringing in suppressed rainfall activity over the southwest quarter. The MJO influence during Northeast Monsoon (NEM) season is reduced as a result of southward shift of the MJO envelope (Salby and Hendon, 1994; Zhang and Dong, 2004; Zhang, 2005) with convective core away from the equator during boreal winter.

Modulation of extreme rainfall events by the MJO over SL is also investigated in this study. These extreme rainfall events can bring serious economic losses with great social damages. Modulation of extreme events by the MJO may play an essential role in the prediction of extreme events, which implies a substantial improvement in planning and preparedness for such events.

Occurrence of extreme events is more frequent during phase 2 in the FIM, phases 2 and 3 in the SWM, phases 1, 2 and 3 in the SIM and phases 2 and 3 in the NEM season. According to Ratnayake and Herath (2005), most of the landslides occur in SL during SIM, SWM and NEM seasons. Southwestern slopes of Rakwana mountain range and western slopes of central hills vulnerable to landslides have a higher chance of occurrence of extreme rainfall events during phases 2 and 3 in SWM season and phase 2 in SIM season respectively. Southeastern slopes of central hills, which are vulnerable to landslides, have higher chance of occurrence of extreme rainfall events during phase 2 in NEM season. There is an enhanced probability of receiving heavy rainfall in flood prone areas in the low lying region in the northeastern and eastern parts during phases 1, 2 and 8 in SIM and in phases 2 and 3 in NEM season and southwest quarter in phase 2 in SWM season. There is a higher chance of occurrence of extreme rainfall events over western parts in phase 3 during NEM season.

This study finds that rainfall variability over SL is greatly influenced by the MJO modulated circulation. The analysis provides a useful reference as to when and where the MJO has significant impacts on SL rainfall variability as well as extreme rainfall events during four climatic seasons. This information can be used along with the accurately predicted MJO phase by dynamical or statistical models, to improve extended range forecasting in SL.

Acknowledgements

Part of this research was undertaken by the first author while hosted at the Bureau of Meteorology through the Endeavour Fellowship program that is funded by the Australian government. We also thank Eun-Pa Lim and Andrew Marshall for their valuable comments. The contents and views expressed in this research paper are the views of the authors and do not necessarily reflects the views of the organizations they belong to.

References

Aldrian, E., 2008, "Dominant Factors of Jakarta's Three Largest Floods", *Journal Hidrosfir Indonesia*, **3**, 105-112.

Barlow, M., Wheeler, M., Lyon, B. and Cullen, H., 2005, "Modulation of Daily Precipitation over Southwest Asia by the Madden-Julian Oscillation", *Monthly Weather Review*, **133**, 3579-3594.

Berhane, F., Zaitchik, B. and Badr, H., 2015, "The Madden-Julian Oscillation's influence on Spring Rainy Season Precipitation over Equatorial West Africa", *Journal of Climate*, **28,** 8653-8672.

Chandimala, J. and Zubair, L., 2007, " Predictability of stream flow and rainfall based on ENSO for water resources management in Sri Lanka", *Journal of Hydrology*, **335**, 303-312.

Chandrapala, L., 1996, "Long Term Trends of Rainfall and Temperature in Sri Lanka" In Y. P. Abrol, S. Gadgil, & G. B. Pant (Eds.), *Climate Variability and Agriculture* (150-152), Narosa Publishing House, New Delhi.

De Silva, C. S., Weatherhead, E. K., Knox, J. W. and Rodriguez-Diaz, J. A., 2007, "Predicting the impacts of climate change - A case study of paddy irrigation water requirements in Sri Lanka", *Agricultural water management*, **93**, 1, 19-29.

Ding, Y. and Sikka, D. R., 2006, "Synoptic systems and weather". In: Wang B (eds.) *The Asian monsoon*. Springer, Berlin, 131-202.

Donald, A., Meinke, H., Power, B., Maia, A. H. N., Wheeler, M. C., White, N., Stone, R. C. and Ribbe, J., 2006, "Near-global impact of the Madden-Julian oscillation on rainfall", *Geophysics Research Letters*, **33**, L09704, doi:10.1029/ 2005GL025155.

Funk, C., Peterson, P., Landsfeld, M., Pedreros, D., Verdin, J., Shukla, S., Husak, G., Rowland, J., Harrison, L., Hoell, A. and Michaelsen, J., 2015, "The climate hazards infrared precipitation with stations - A new environmental record for monitoring extremes", *Scientific data*, **2**, 150066.

Gottschalck, J., Wheeler, M. , Weickmann, K., Vitart, F., Savage, N., Lin, H., Hendon, H., Waliser, D., Sperber, K., Nakagawa, M., Prestrelo, C., Flatau, M. and Higgins, W., 2010, "A framework for assessing operational Madden-Julian Oscillation forecasts : A CLIVAR MJO Working Group project", *Bulletin of the American Meteorological Society*, **91**, 1247-1258.

Ichikawa, H. and Yasunari, T., 2008, "Intraseasonal variability in diurnal rainfall over New Guinea and the surrounding oceans during austral summer", *Journal of Climate*, **21**, 2852-2868.

India Meteorological Department, 1973, "Northeast monsoon", FMU Report No. IV-18.4.

Jia, X., Chen, L., Ren, F. and Li, C., 2010, "Impacts of the MJO on winter rainfall and circulation in China", *Advances in Atmospheric Sciences*, **28**, 521-533.

Jones, C. and Carvalho, L. M. V., 2012, "Spatial-Intensity Variations in Extreme Precipitation in the Contiguous United States and the Madden-Julian Oscillation", *Journal of Climate*, **25**, 4849-4913.

Jones, C., Waliser, D. E., Lau, K. M. and Stern, W., 2004, "Global occurrences of extreme precipitation events and the Madden-Julian oscillation: Observations and predictability", *Journal of Climate*, **17**, 4575-4589.

Kalnay, E., Kanamitsu, M., Kistler, R., Collins, W., Deaven, D., Gandin, L., Iredell, M., Saha, S., White, G., Woollen, J. and Zhu, Y., 1996, "The NCEP/NCAR 40-Year Reanalysis Project", *Bulletin of the American Meteorological Society*, **77**, 437-471.

Kane, R. P., 1998, "ENSO relationship to the rainfall of Sri Lanka", *International Journal of Climatology*, **18**, 8, 859-872.

Lee, J. Y., Wang, B., Wheeler, M. C., Fu, X., Waliser, D. E. and Kang, I. S., 2013, "Real-time multivariate indices for the boreal summer intra- seasonal oscillation over the Asian summer monsoon region", *Climate Dynamics*, **40**, 493-509.

Liebmann, B. and Smith, C. A., 1996, "Description of a complete (interpolated) outgoing longwave radiation dataset", *Bulletin of American Meteorology Society*, **77**, 1275-1277.

Madden, R. A. and Julian, P. R., 1971, "Detection of a 40-50 day oscillation in the zonal wind in the tropical Pacific", *Journal of the Atmospheric Sciences*, **28**, 702-708.

Madden, R. A. and Julian, P. R., 1972, "Description of global-scale circulation cells in the tropics with a 40-50 day period", *Journal of the Atmospheric Sciences*, **29**, 1109-1123.

Madden, R. A. and Julian, P. R., 1994, "Observations of the 40-50-day tropical oscillation: A review", *Monthly Weather Review*, **122**, 814-837.

Malmgren, B. A., Hulugalla, R., Hayashi, Y. and Mikami, T., 2003, "Precipitation trends in Sri Lanka since the 1870s and relationships to El Niño-Southern Oscillation", *International Journal of Climatology*, **23**, 10, 1235-1252.

Marshall, A. G., Hudson, D., Wheeler, M. C., Hendon, H. H. and Alves, O., 2012, "Simulation and prediction of the MJO and its teleconnections using POAMA", In Understanding and Prediction of Monsoon Weather and Climate-abstracts of the sixth CAWCR Workshop 12 November-15 November, 2012, Melbourne, Australia CAWCR Technical Report 056, 113-116.

Martin, E. R. and Schumacher, C., 2011, "Modulation of Caribbean precipitation by the Madden-Julian oscillation", *Journal of Climate*, **24**, 3, 813-824.

Matthews, A. J., Pickup, G., Peatman, S. C., Clews, P. and Martin, J., 2013, "The effect of the Madden-Julian Oscillation on station rainfall and river level in the Fly River system, Papua New Guinea", *Journal of Geophysics Research-Atmosphere*, **118**, 10,926-10,935, doi:10.1002/jgrd.50865.

Meinke, H. and Stone, R. C., 2005, "Seasonal and inter-annual climate forecasting: The new tool for increasing preparedness to climate variability and change in agricultural planning and operations", *Climatic Change*, **70**, 221-253.

Nakazawa, T., 1988, "Tropical super clusters within intraseasonal variations over the western Pacific", *Journal of the Meteorological Society of Japan*, **66,** 823-839.

Neena, J. M., Lee, J. Y., Waliser, D., Wang, B. and Jiang, X., 2014, "Predictability of the Madden-Julian Oscillation in the Intraseasonal Variability Hindcast Experiment (ISVHE)", *Journal of Climate*, **27**, 4531-4543.

Pai, D. S., Bhate, J., Sreejith, O. P. and Hatwar, H. R., 2011, "Impact of MJO on the intraseasonal variation of summer monsoon rainfall over India", *Climate Dynamics*, **36**, 41-55. DOI 10.1007/s00382-009-0634-4.

Peatman, S. C., Matthews, A. J. and Stevens, D. P., 2014, "Propagation of the Madden-Julian Oscillation through the Maritime Continent and scale interaction with the diurnal cycle of precipitation", *Quarterly Journal of Royal Meteorological Society*, **140**, 814-825. DOI:10.1002/qj.2161

Pohl, B. and Camberlin, P., 2006, "Influence of the Madden-Julian oscillation on east African rainfall. I : Intraseasonal variability and regional dependency", *Quarterly Journal of Royal Meteorological Society*, **132**, 2521-2539, DOI:10.1256/ qj.05.104.

Punyawardena, B. V. R. and Cherry, N. J., 1999, "Assessment of the predictability of the seasonal rainfall in Ratnapura using southern oscillation and its two extremes", *Journal of the National Science Council of Sri Lanka*, **27**, 3, 187-195.

Rashid, H. A., Hendon, H. H., Wheeler, M. C. and Alves, O., 2011, "Prediction of the Madden-Julian oscillation with the POAMA dynamical prediction system", *Climate Dynamics*, **36**, 649-661.

Rasmusson, E. M. and Carpenter, T. H., 1983, "The relationship between eastern equatorial Pacific sea surface temperature and rainfall over India and Sri Lanka", *Monthly Weather Review*, **110**, 354-383.

Ratnayake, U. and Herath, S., 2005, "Changing rainfall and its impact on landslides in Sri Lanka", *Journal of Mountain Science*, **2**, 218-224.

Rauniyar, S. P., Protat, A. and Kanamori, H., 2017, "Uncertainties in TRMM-Era multisatellite-based tropical rainfall estimates over the Maritime Continent", *Earth and Space Science*, **4**, 275-302, doi:10.1002/2017EA000279.

Ropelewski, C. F. and Halpert, M. S., 1987, "Global and regional scale precipitation patterns associated with the El Niño/southern oscillation", *Monthly Weather Review*, **115**, 1606-1626.

Ropelewski, C. F. and Halpert, M. S., 1989, "Precipitation patterns associated with the high index phase of the southern oscillation", *Journal of Climate*, **2**, 3, 268-284.

Salby, M. L. and Hendon, H. H., 1994, "Intraseasonal behavior of clouds, temperature and motion in the tropics", *Journal of the Atmospheric Sciences*, **51**, 2207-2224.

Shiryaev, A. N., 1996, "Probability", No. 95 in Graduate Texts in Mathematics. 2nd ed. Springer-Verlag, p621.

Slingo, J., Inness, P., Neale, R., Woolnough, S. and Yang, G. Y., 2003, "Scale interactions on diurnal to seasonal timescales and their relevance to model systematic errors", *Annals of* Geophysics, **46**, 139-155.

Somasekeram, T., Perera, L. A. G., Perera, M. P., De Silva, B. G., Karunanayake, M. M. and Epitawatta, D. S., 1988, *National Atlas.* Survey Department : Colombo.

Sumathipala, W. L. and Punyadeva, N. B. P., 1998, "Variation of the rainfall of Sri Lanka in relation to El Nino", Proceedings of the 14th Technical Session of the Institute of Physics, Colombo, Sri Lanka, 12-19.

Suppiah, R. and Yoshino, M. M., 1984, "Rainfall variations of Sri Lanka part 1 : Spatial and temporal patterns", *Archives for meteorology, geophysicsand bioclimatology*, Series B, **34**, 4, 329-340.

Suppiah, R. and Yoshino, M. M., 1986, "Some agroclimatological aspects of rice production in Sri Lanka", *Geographical Review of Japan*, Series B, **59**, 2, 137-153.

Suppiah, R., 1989, "Relationships between the southern oscillation and the rainfall of Sri Lanka", *International Journal of Climatology*, **9**, 6, 601-618.

Suppiah, R., 1996, "Spatial and temporal variations in the relationship between the southern oscillation and the rainfall of Sri Lanka", *International Journal of Climatology*, **16**, 12, 1391-1407.

Suppiah, R., 1997, "Extremes of the southern oscillation and the rainfall of Sri Lanka", *International Journal of Climatology*, **17**, 1, 87-101.

Tangang, F. T., Juneng, L., Salimun, E., Vinayachandran, P. N., Seng, Y. K., Reason, C. J., Behera, S. K. and Yasunari, T., 2008, "On the roles of the northeast cold surge, the Borneo vortex, the Madden-Julian Oscillation and the Indian Ocean Dipole during the extreme 2006/2007 flood in southern Peninsular Malaysia", *Geophysics Research Letters*, **35,** L14S07, doi:10.1029/ 2008GL033429.

Thambyahpillay, G., 1954, "The rainfall rhythm in Ceylon", *The University of Ceylon Review*, **12**, 4, 223-274.

Vialard, J., Terray, P., Duvel, J. P., Nanjundiah, R. S., Shenoi , S. S. and Shankar, D., 2011, "Factors controlling January–April rainfall over southern India and Sri Lanka", *Climate Dynamics*, **37,** 493-507.

Waliser, D., 2005, "Predictability and forecasting", *Intraseasonal Variability in the Atmosphere-Ocean Climate System*, W. K. M. Lau and D. E. Waliser, Eds., Springer-Verlag, 389-423.

Wheeler, M. C. and Hendon, H. H., 2004, "An all-season real-time multivariate MJO index: Development of an index for monitoring and prediction", *Monthly Weather Review*, **132**, 1917-1932.

Wheeler, M. C., Hendon, H., Cleland, S., Donald, A. and Meinke, H., 2009, "Impacts of the Madden - Julian oscillation on Australian rainfall and circulation", *Journal of Climate*, **22**, 1482-1498.

Wilks, D. S., 2006, "Statistical Methods in the Atmospheric Sciences", *Academic Press*, p648.

Yoshino, M. M. and Suppiah, R., 1983, "Climate and paddy production: a study on selective districts in Sri Lanka", In *Climate, Water and Agriculture in Sri Lanka*, *Climatological Notes*, **33**, 33-50.

Zhang, C. andDong, M., 2004, "Seasonality of the Madden-Julian oscillation", *Journal of Climate*", **17**, 3169-3180.

Zhang, C., 2005, "Madden-Julian Oscillation", *Reviews of Geophysics*, **43,** RG2003, doi:10.1029/2004RG000158.

Zhang, C., 2013, "Madden-Julian oscillation: Bridging weather and climate", *Bulletin of the American Meteorological Society*, **94**, 1849-1870.

Zhang, L. N., Wang, B. Z. and Zeng, Q. C., 2009, "Impacts of the Madden-Julian Oscillation on Summer Rainfall in Southeast China", *Journal of Climate*, **22**, 201-216.

Zhu, C., Nakazawa, T., Li, J. and Chen, L., 2003, "The 30-60 day intraseasonal oscillation over the western North Pacific Ocean and its impacts on summer flooding in China during 1998", *Geophysics Research Letters*, **30**, 18.

Zubair, L. and Ropelewski, C. F., 2006, "The Strengthening Relationship between ENSO and Northeast Monsoon Rainfall over Sri Lanka and Southern India", *Journal of Climate*, **19**, 1567-1575.